Chemical Physics Letters 745 (2020) 137236

Contents lists available at ScienceDirect

Chemical Physics Letters

journal homepage: www.elsevier.com/locate/cplett

Research paper

Theoretical study of greenhouse gases on the zirconium oxide nanotube surface

José Antônio Pinheiro Lobo[a], Jeziel Rodrigues dos Santos[a,*], Osmair Vital de Oliveira[b,*], Elson Longo da Silva[c], José Divino dos Santos[a]

[a] Goias State University, Anápolis Campus, Zip Code: 75.132-903, GO, Brazil
[b] Federal Institute of Education, Science and Technology of São Paulo, Catanduva Campus, Zip Code: 15.808-305, Catanduva, SP, Brazil
[c] INCTMN, LIEC, Department of Chemistry, Federal University of São Carlos, Zip Code: 13.565-905, São Carlos, SP, Brazil

HIGHLIGHTS

- DFT method was used to study the adsorption of pollutant gases by SWZNT.
- SWZNT electrical conductivity is improved by $CFCl_3$ adsorption.
- $CFCl_3$ adsorption by BNNT is more favorable than CO_2 and CH_4 molecules.
- SWZNT can be a new gas sensor for $CFCl_3$ gas detection and its derivatives.

ARTICLE INFO

Keywords:
Greenhouse gas sensor
Zirconium oxide nanotube
DFT

ABSTRACT

Herein, density functional theory was used to investigate the zirconium oxide nanotube (SWZNT-c(1 1 1)) as a possible candidate for detection of greenhouse gases such as $CFCl_3$, CO_2 and CH_4. The results indicate that SWZNT-c(1 1 1) has an energy gap selectivity for the $CFCl_3$ molecule, increasing its electrical conductivity by ~16.17%. This interaction causes a displacement of LUMO energy, causing the SWZNT-c (1 1 1)/$CFCl_3$ hardness (η) complex to have the greatest decrease, proving the greatest reactivity of $CFCl_3$. Therefore, based in these favorable properties and the lowest adsorption energy imply that the SWZNT-c(111 can be used as a promising $CFCl_3$ sensor.

1. Introduction

In recent years, computational theoretical chemistry has been presented as one of the main tools for the structural and electronic study of nanometric compounds, in order to help the development of new materials, facilitating thereby the understanding and applications of these materials in different branches such as the development of materials with photocatalytic properties [1–4], materials with environmental applications [5], materials with antibacterial and fungicidal actives [6], as well as the development of new sensors [7–10]. Among these, we highlight the materials formed by elements belonging to group IV, such as Ti, Zr, Hf [11], because they have mechanical resistance and also at high temperatures [12].

The Zirconia (ZrO_2) is considered one of the most important ceramic materials due to its properties, because it has high mechanical and thermal resistance, also has high radiation resistance and can be effectively applied in the nuclear industry [13]. Under normal pressure conditions, zirconia has three temperature controlled polymorphs, at temperatures above 2350 °C the cubic phase predominates, while at temperatures below 1150 °C the predominant phase is the monoclinic and as intermediate between the two. In two phases, there is tetragonal morphology [13].

With the advances obtained through the synthesis of carbon nanotubes [14], a new research field of materials has been opened, aiming to synthesize new nanotubular structures from inorganic compounds, which in turn, have properties independent of their chirality since theoretical and experimental advances showed that carbon nanotubes had properties dependent on their chirality [15]. Between the so-called inorganic nanotubes, are ZrO_2 nanotubes, successfully synthesized by the anodizing method [16], as well as electrofiation, solution-based deposition, among others [17], and these nanotubes can have a variety of applications, such as host matrix for optical functional materials,

* Corresponding authors.
E-mail addresses: jeziel_chess@hotmail.com (J. Rodrigues dos Santos), osmairvital@gmail.com (O. Vital de Oliveira).

https://doi.org/10.1016/j.cplett.2020.137236
Received 1 February 2020; Received in revised form 10 February 2020; Accepted 15 February 2020
Available online 17 February 2020
0009-2614/

solid oxide fuel cell electrolytes and gas sensing components [17].

Regarding to theoretical studies reported in the literature, two studies have been found so far that report the stability of ZrO_2 nanotubes, in which periodic calculations are performed for different structures in different morphologies [18], as well as the estimation of the modulus of ZrO_2 Young is reported [19]. Until now, no theoretical reports of interactions with greenhouse gases have been found in the literature, such as trichloromonofluormethane ($CFCl_3$), carbon dioxide (CO_2) and methane gas (CH_4). It is interesting to point that recently theoretical methods were used to study the adsorption of various toxic gases in different nanomaterials such as Rh-doped $MoSe_2$ monolayer [20], Ni-doped InN monolayer [21] and many others as cited by Cui [22].

Therefore, observing the lack of literature on computational theoretical studies regarding ZrO_2 nanotubes, this work aims to present a study of the interaction of greenhouse gas molecules on the outer surface of ZrO_2 nanotubes. In this way, the density fuctional theory (DFT) was ued to analyse the formation energies of the complexes, as well as modifications of the structural and electronic properties of the material, contributing to the advance in the studies of new gases sensors based in the ZrO_2 nanotubes.

2. Methodology

2.1. Obtaining the crystalline plane (1 1 1) from cubic morphology.

The crystalline plane (1 1 1) formed by the cubic phase was based on the unit cell of ZrO_2 cubic morphology, considering the lattice parameters, a = b = c = 5,0 Å and α = β = γ = 90°. A ZrO_2 cubic unit cell model was constructed using the Cartesian coordinates of atoms as a function of the network parameters (a, b and c). The table 1 presents the fractional coordinates of atoms in the unit cell of cubic morphology of ZrO_2. From the unit cell, it was possible to represent the crystalline structure of ZrO_2 in the cubic morphology modeled by applying translation operations to the Cartesian coordinates of atoms.

The plane (1 1 1) was modeled from the ZrO_2 unit cell, establishing a basic unit of repetition that, when translated, generated the plane to be studied, reproducing the coordinates of the atoms of Zr and O in the plane. The basic unit of repetition was determined from the coordinates of the Zr and O atoms that belonged to the studied plane, maintaining the stoichiometry (1:2) between the Zr and O atoms, as shown in Fig. 1. Fig. 1 presents a representation of the structure.

The translations of the basic unit were performed by applying translation matrices at the coordinates (x; y; z) of all atoms. Horizontal translations occurred along the xy plane, applying the translation

Table 1
Fractional coordinates of Zr and O atoms in ZrO_2 unit cell.

Atoms	a (Å)	b (Å)	c (Å)
Zr	0	0	0
Zr	$\frac{1}{2}$	$\frac{1}{2}$	0
Zr	$\frac{1}{2}$	0	$\frac{1}{2}$
Zr	0	$\frac{1}{2}$	0
O	$\frac{1}{4}$	$\frac{3}{4}$	$\frac{1}{4}$
O	$\frac{3}{4}$	$\frac{1}{4}$	$\frac{1}{2}$
O	$-\frac{1}{4}$	$\frac{3}{4}$	$\frac{1}{4}$
O	$\frac{1}{4}$	$\frac{1}{4}$	$\frac{1}{4}$
O	$\frac{1}{4}$	$\frac{1}{4}$	$\frac{3}{4}$
O	$-\frac{1}{4}$	$\frac{3}{4}$	$\frac{3}{4}$
O	$\frac{3}{4}$	$\frac{1}{4}$	$-\frac{1}{4}$
O	$\frac{1}{4}$	$\frac{3}{4}$	$-\frac{1}{4}$

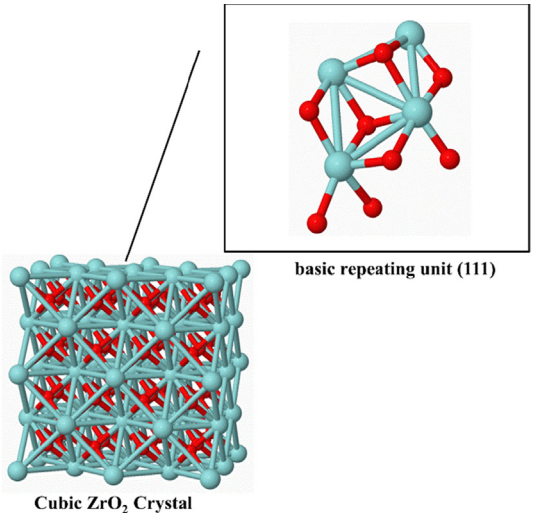

Fig. 1. Structures of the basic repetition unit taken from the ZrO_2 crystal in the cubic phase. Zirconium in cyan and oxygen in red. (For interpretation of the color references in this figure caption, the reader is consulted on the web version of this article).

matrix represented in Eq. (1).

$$[x' \quad y' \quad z'] = [x \quad y \quad z]\begin{bmatrix} 1000 \\ 0100 \\ 0010 \\ dxdydz1 \end{bmatrix} \tag{1}$$

where x, y and z are the initial coordinates of the atoms, x ', y' and z 'are the coordinates of the atoms after translation and dx, dy and dz correspond to the translation distances in the x, y and z directions of the Cartesian system. By performing the operations indicated in the conversion matrix indicated in Eq. (1), Eq. (2) is obtained.

$$\begin{cases} x' = x + dx \\ y' = y + dy \\ z' = z + dz \end{cases} \tag{2}$$

For horizontal translations, the value of dx corresponds to the value of the negative network parameter (a) (-a), the value of dy corresponds to the value of the positive network parameter (b) and the value of dz is zero. To increase the number of levels (m), Eq. (2) was also applied. To increase the number of levels (m) of the plane (1 1 1), a value of dx equal to a negative network parameter (-a), a value of dy equal to zero and a value of dz equal to a network positive (c) for each level added.

After modeling the plane, they were translated to the origin of the Cartesian system and rotated to the xz plane, applying translation and rotation matrices to generalize the plane curvature process and criate ZrO_2 nanotube models. Accomplishmenting the translation, the translation matrix presented in Eqs. (1) and (2) was again used, with values of dx equal to the negative network parameter (-a) and values of dy and dz equal to zero. To perform the rotation around the z axis (RZ), was used a rotation matrix presented in Eq. (3).

$$[x'' \quad y'' \quad z''] = [x' \quad y' \quad z']\begin{bmatrix} cos\varphi sen\varphi 00 \\ -sen\varphi cos\varphi 00 \\ 0010 \\ 0001 \end{bmatrix} \tag{3}$$

where x', y' and z'correspond to atomic coordinates after translation and x", y" and z"correspond to atomic coordinates after translation and rotation in z (RZ), φ corresponds to the 45° rotation angle for this operation, since the plane (1 1 1) was modeled at 45° between the × and y axes, and the basic repetition unit was moved in the negative direction of x. Performing the operations indicated in Eq. (3), Eq. (4) was obtained.

$$\begin{cases} x'' = x'cos\varphi - y'sen\varphi \\ y'' = x'sen\varphi + y'cos\varphi \\ z'' = z' \end{cases} \quad (4)$$

Replacing Eq. (2) into Eq. (4), gets Eq. (5), which allows the final coordinates to be related to the initial coordinates of the atoms, making it possible to execute the operation directly.

$$\begin{cases} x'' = (x + dx)cos\varphi - (y + dy)sen\varphi \\ y'' = (x + dx)sen\varphi + (y + dy)cos\varphi \\ z'' = z + dz \end{cases} \quad (5)$$

To reorient the plane model (1 1 1) it was necessary to make an additional rotation, applied around the x-axis (RX) at an angle of −56°, because the crystallographic plane (1 1 1) has a greater inclination than for example applied to the plan (1 1 0). To perform the rotation around the × axis (RX), the rotation matrix represented in Eq. (6) was used.

$$[x''' \quad y''' \quad z'''] = [x'' \quad y'' \quad z''] \begin{bmatrix} 0000 \\ 0cos\varphi sen\varphi 0 \\ 0 - sen\varphi cos\varphi 0 \\ 0001 \end{bmatrix} \quad (6)$$

where x''', y''' and z''' represent the coordinates of atoms in the xz plane, x'', y'' and z'' represent the coordinates after rotation in × (RX) and φ represents the angle of rotation employed, −56°. Performing the operations indicated in Eq. (6) gets Eq. (7).

$$\begin{cases} x''' = x'' \\ y''' = x''cos\varphi - z''sen\varphi \\ z''' = y''sen\varphi + z''cos\varphi \end{cases} \quad (7)$$

2.2. Obtaining Z-direction nanotube models.

With the crystalline planes (1 1 1) already repositioned in the xz plane of the Cartesian system, they were converted to the cylindrical shape, bending them 360°. To obtain the cylindrical structure by applying the rotation with respect to the z axis, Eq. (8) is defined, where the perimeter (pe) of the structure is equal to the length of the modeled plane (pl) plus the distance of a bond between the atoms of Zr and O (lb).

$$pe = pl + lb \quad (8)$$

where the length of the plane (pl) can be calculated according to Eq. (9).

$$pl = n\sqrt{(a^2 + b^2)} \quad (9)$$

where (n) corresponds to the number of horizontal repeating units of the modeled plane and the term $\sqrt{(a^2 + b^2)}$ corresponds to the length of the unit cell.

The length of a bond (lb) between the atoms of Zr and O has been inserted so that the atoms do not overlap during the process of forming nanotube models. To convert the ZrO_2 crystal plane models to cylindrical structures, the coordinates of the crystal plane atoms were transformed into polar coordinates using Eq. (10).

$$\begin{cases} xp = rcos\varphi \\ yp = rsen\varphi \\ zp = z \end{cases} \quad (10)$$

where xp, yp and zp correspond to the polar coordinates, φ corresponds to the angle of rotation and r is the radius of the atom in the obtained nanotube model. The atoms of the modeled surfaces of ZrO_2 are not in the same plane; therefore, when they are transformed into cylindrical structures, there are variations in the radius length of atoms in the structure; therefore, the value of r in Eq. (10) is calculated individually for atoms.

The radius value was obtained considering the average radius of the structure. The average radius corresponds to the radius formed by atoms in the crystalline plane. For atoms that are out of the plane, the radius value is adjusted according to the y coordinate, so that the radius value can be calculated according to Eq. (11), considering the geometric formula for converting a flat rectangular surface to a cylinder plus the y coordinate of the plane.

$$r = \frac{pe}{2\pi} + y \quad (11)$$

The angle (φ) that corresponds to the angle between the initial × coordinate in the plane to be rotated and the atom coordinate in the nanotube model can be obtained from Eq. (12).

$$\varphi = \frac{2\pi x}{pe} \quad (12)$$

The equations obtained through this methodology were inserted in an internal script, written in programming language, generalizing thereby the obtaining of the models.

3. Computational details

The initial structure of SWZNT-c(1 1 1) in cubic morphology, consisting of 48 zirconium atoms and 96 oxygen atoms, was constructed using a script written internally using the methodology presented in sections 2.1 and 2.2. This nanotube model has d1 = 13.49, d2 = 11.45 and 10.66 Å in diameters and length, respectively. For the complexes, the initial configurations were constructed by placing the molecules of ($CFCl_3$, CO_2 and CH_4) in different regions around the surface of SWZNT-c(1 1 1). The molecules (CFCl3, CO_2 and CH_4), SWZNT-c(1 1 1) and the complexes (SWZNT-c (1 1 1)/$CFCl_3$, SWZNT-c (1 1 1)/CO_2 and SWZNT-c(1 1 1)/CH_4) were initially optimized with Hamilton PM7 using the MOPAC2016 program [23]. Posteriorly, the structures with minimum energies were re-optimized with DFT calculations, considering the functional B3LYP hybrid with the 3-21G [24]. The dispersion interaction correction was take in account using the Grimme's method (GD3) [25]. This procedure was chosen to balance the computational cost and the quality of the results, since the Zr atom does not have a larger base set. The stationary points were characterized as a minimum energy point using harmonic vibrational states, which were not observed frequencies. All DFT calculations were performed under vacuum using the Gaussian 09 package [26]. The orbital natural bonding method (NBO) [27] was used to calculate atomic charges. The adsorption energy (E_{ad}) of the complex was calculated using Eq. (13).

$$E_{ad} = E_{complex} - (E_{nanotube} + E_{molecule}) \quad (13)$$

where, $E_{complex}$ is the total energy of the complexes (SWZNT-c (1 1 1)/$CFCl_3$, SWZNT-c (1 1 1)/CO_2 and SWZNT-c (1 1 1)/CH_4), $E_{nanotube}$ is the total energy of SWZNT-c(1 1 1) and $E_{molecule}$ is the total energy of molecules ($CFCl_3$, CO_2 and CH_4).

4. Results and discussion

4.1. Structural analysis

At this current work, the DFT method was used to study SWZNT-c (1 1 1) with the intention of obtaining a new sensor to identify the presence of polluting gases such as $CFCl_3$, CO_2 and CH_4. Fig. 2 presents the optimized structures with minimum energy obtained in the DFT method. Overall, as can be seen in Fig. 2, no significant structural change in SWZNT-c (1 1 1) was observed after complex formation.

For the complexes, a shorter bond length (0.245 nm) between fluorine and zirconium atom ($CFCl_3$) was observed. For the interactions with (CO_2) and (CH_4), this length was, respectively, 0.285 (oxygen and zirconium) and 0.314 nm (hydrogen and oxygen). From NBO analysis, it was confirmed that $CFCl_3$ fluorine is more strongly bound to the

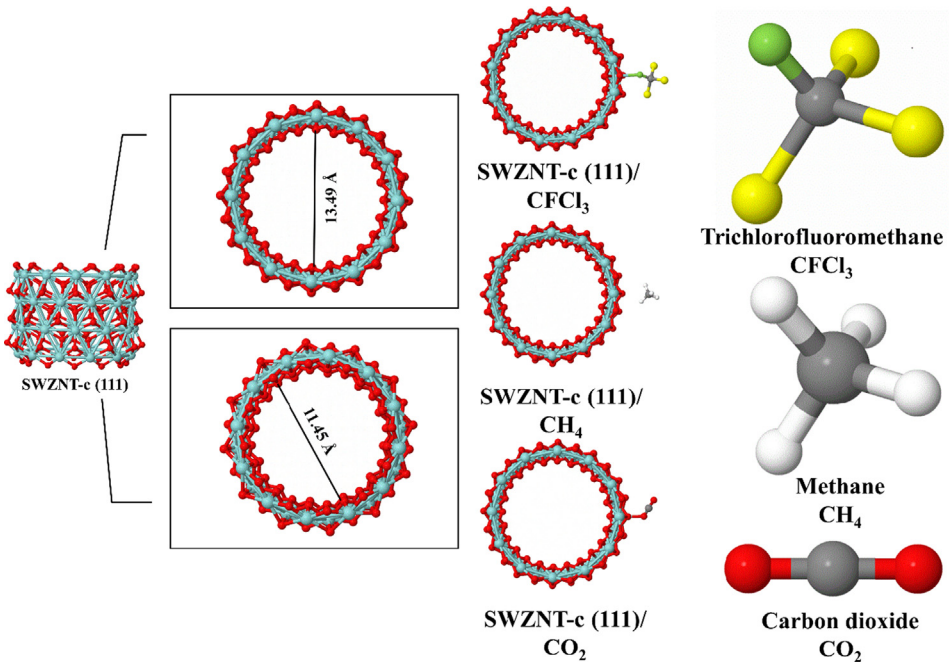

Fig. 2. Studied structures optimized with the DFT//B3LYP/3-21G/GD3 method. Oxygen in red, zirconium in cyan, carbon in gray, hydrogen in white, fluorine in green and chlorine in yellow. (For interpretation of the color references in this caption, the reader is consulted on the web version of this article).

Table 2
Electronic properties calculated using DFT//B3LYP/3-21G/GD3.

Properties	$CFCl_3$	CO_2	CH_4	SWZNT-c (1 1 1)	SWZNT-c (1 1 1)/$CFCl_3$	SWZNT-c (1 1 1)/CO_2	SWZNTc (1 1 1)/CH_4
$\varepsilon_{HOMO}(eV)$	− 9.09	−9.62	−10.58	−7.83	−7.79	−7.81	−7.83
$\varepsilon_{LUMO}(eV)$	−2.88	0.65	3.97	−2.82	−3.59	−2.80	−2.81
E_g [a]	6.21	8.97	6.61	5.01	4.20	5.01	5.00
$\Delta E_{formation}$ [b]	–	–	–	−7645.52	–	–	–
E_{ad} [b]	–	–	–	–	–33.08	−24.58	−4.43
dipole moment [c]	0.09	0.00	0.00	9.70	10.04	9.94	9.67
I (eV)	9.09	9.62	10.58	7.83	7.79	7.81	7.83
A (eV)	2.88	−0.65	−3.97	2.82	3.59	2.80	2.81
η (eV)	7.65	9.95	12.57	6.42	6.00	6.41	6.43
X (eV)	10.53	9.30	8.60	9.24	9.59	9.21	9.24
μ (eV)	−5.99	−4.49	−3.31	−5.33	−5.69	−5.31	−5.32
ω (eV)	2.35	1.01	0.44	2.21	2.70	2.20	2.20
S (eV)	0.07	0.05	0.04	0.08	0.08	0.08	0.08

[a] $\varepsilon_{HOMO} - \varepsilon_{LUMO}$at eV.
[b] at kcal/mol.
[c] at Debye.

SWZNT-c(1 1 1) Zr atom with a binding order of 0.890, followed by the CO_2 oxygen atom with a binding order of 0.727 while that the hydrogen atoms of CH_4 have a surface bond order of SWZNT-c(1 1 1) equivalent to 0.04. In the next section, the electronic structures for compounds and complexes are presented and discussed to understand the energetic process involved.

4.2. Electronic structure

The electronic properties were used to clarify the chemosorption process of $CFCl_3$, CO_2 and CH_4 molecules on the surface of SWZNT-c (1 1 1). Initially, it is important to evaluate the stability of the obtained SWZNT-c(1 1 1) model, which can be treated by the formation energy ($\Delta E_{formation}$) using Eq. (14).

$$\Delta E_{formation} = E_{SWZNT\text{-}c(111)} - -(4mn(E_{ZrO2})) \quad (14)$$

where $E_{SWZNT\text{-}c\ (1\ 1\ 1)}$ is the total energy of the nanotube, "n" is the basic repetition unit number, "m" is the number of nanotube levels, and E_{ZrO2} is the total energy of ZrO_2. The ΔEformation value for SWZNT-c (1 1 1) was −7645.52 kcal/mol, being energetically favorable in its formation and in accordance with the calculations performed by Bandura and Evarestov [18]. Table 2 summarizes some important electronic properties obtained and discussed here.

The reactivity parameters were based on the energies of the highest energy occupied molecular orbitals (HOMO, ε_{HOMO}) and the energies of the lowest energy unoccupied molecular orbitals (LUMO, ε_{LUMO}). For example, according to Koopmans' theorem [28], the ionization potential (I) is described in the negative energy of HOMO, and the electronic affinity (A) can be approximated by the energy of the LUMO opposite signal. The energy gap (for example) is an important property obtained through these two reactivity parameters, being defined as the difference between HOMO and LUMO energies in modulus. Besides that, quantum molecular descriptors such as global hardness (η), electronegativity (χ), electronic chemical potential (μ), electrophilicity (ω) and softness chemistry (S) can be approximated by Eqs. (15)–(19) respectively. [29], where the values are reported in Table 2.

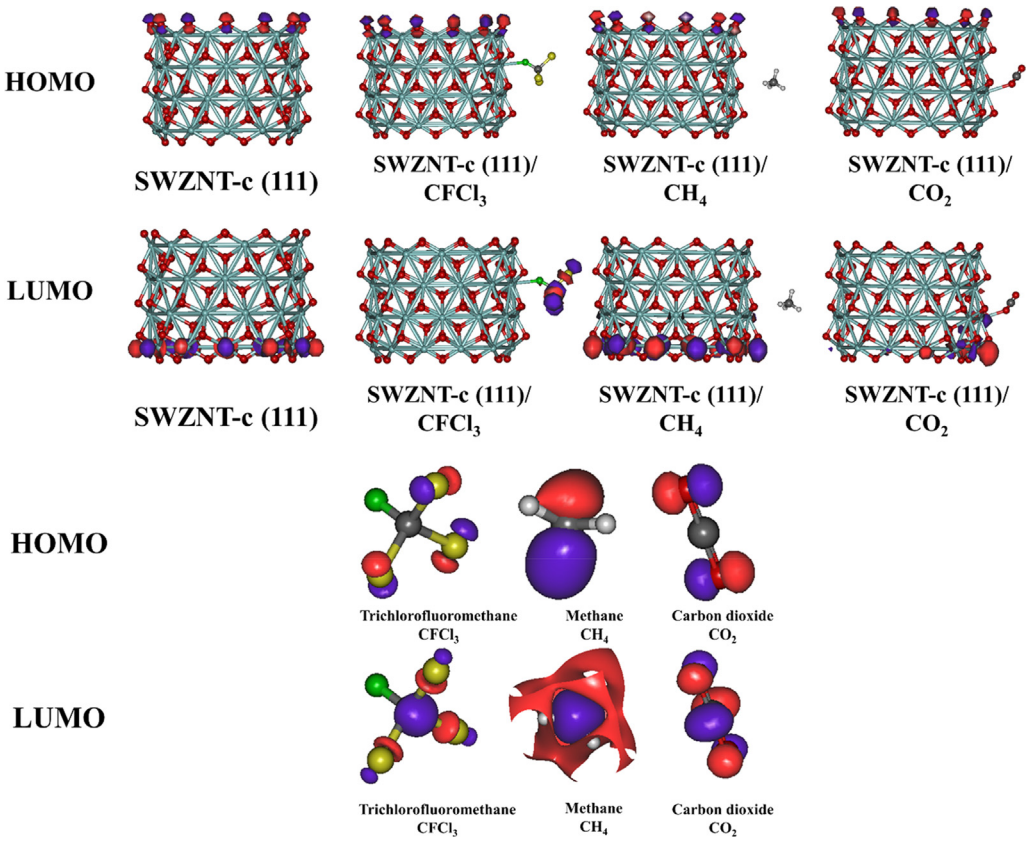

Fig. 3. Representation of the HOMO and LUMO energies of the SWZNT-c(1 1 1) and molecules ($CFCl_3$, CO_2 and CH_4).

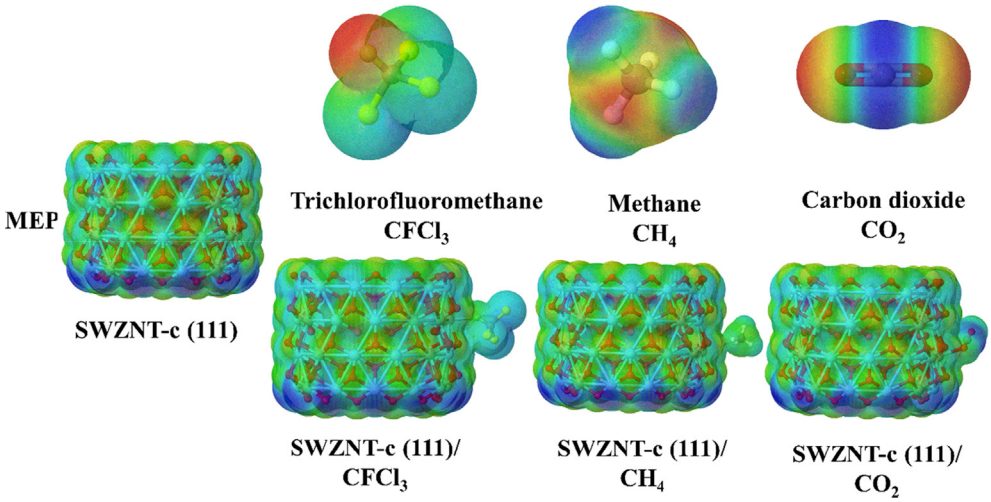

Fig. 4. Representation of the electrostatic molecular potential (MEP, in eV) of SWZNT-c(1 1 1) and molecules ($CFCl_3$, CO_2 and CH_4). For MEP, negative and positive charges range from red to blue, respectively. (For interpretation of the color references in this figure caption, the reader is consulted on the web version of this article).

$$\eta = I - \frac{A}{2} \tag{15}$$

$$\chi = I + \frac{A}{2} \tag{16}$$

$$\mu = -\frac{(I + A)}{2} \tag{17}$$

$$\omega = \frac{\mu^2}{2\eta} \tag{18}$$

$$S = \frac{1}{2\eta} \tag{19}$$

The large and small values of E_g imply a high stability and reactivity, respectively, of a compound in a chemical reaction. Therefore, CO_2 is the most stable compound studied here with a value of 8.97 eV and lower electron affinity (A). The same way, the large energy gap (5.01 eV) that SWZNT-c(1 1 1) presents indicates an insulating material, which in turn agrees with the literature [18], which are reported ZrO_2 nanotubular structures with gap between 5 and 6 eV.

Furthermore, the stability of molecular systems is related to the hardness (η), which is a tool for understanding chemical reactivity [30]. As shown in table 2, the global hardness value (η) for SWZNT-c(1 1 1) is 6.42 eV and after complex formation (SWZNT-c (1 1 1)/$CFCl_3$, SWZNT-c (1 1 1)/CO_2 and SWZNT-c(1 1 1)/CH_4) is changed to 6.00, 6.41 and 6.43 eV, respectively. The results indicate that the value of (η) of SWZNT-c (1 1 1) decreases with the interactions of the molecules and

the reactivity with $CFCl_3$ is higher when compared with CO_2 and CH_4. The electronic chemical potential (μ) of the (SWZNT-c (1 1 1)/$CFCl_3$ complex also decreased. So the (SWZNT-c (1 1 1)/$CFCl_3$) complex has high chemical activity, low chemical stability and is a softness system.

The dipole moment value of (SWZNT-c(1 1 1) is increased by the chemosorption of the $CFCl_3$ and CO_2 molecules from 9.70 Debye to 10.04 and 9.94 Debye in the complexes (SWZNT-c(1 1 1)/$CFCl_3$, SWZNT-c(1 1 1)/CO_2), respectively, and the structure dipole moment value (SWZNT-c(1 1 1) is decreased by the interaction of CH_4 from 9.70 to 9.67 Debye in the SWZNT-c(1 1 1)/CH_4) (see Table 2). The change in dipole moment after interaction with the surface of SWZNT-c(1 1 1) indicates a charge transfer between the molecules ($CFCl_3$, CO_2 and CH_4) and the ZrO2 nanotubes. This trend of charge transfer can be evidenced by the charge analysis in the NBO method, and for the SWZNT-c(1 1 1) the interacting Zr atom has an atomic charge of 1,34e$^-$, while analyzing the same atom after interaction it is noticed that it reduces its atomic charge to 1.22 and 1,31e$^-$ for the complexes formed with $CFCl_3$ and CO_2, respectively.

Consequently, as expected, the strongest interactions were observed between SWZNT-c(1 1 1) and $CFCl_3$ and CO_2 molecules, as shown in Fig. 2. The E_{ad} values (Table 2) follow the order: $-3.08 < -24.58 < -4.43$ kcal/mol for (SWZNT-c(1 1 1)/$CFCl_3$, SWZNT-c(1 1 1)/CO_2 and SWZNT-c(1 1 1)/CH_4), respectively. The higher E_{ad} value for SWZNT-c(1 1 1)/CH_4 indicates a physical adsorption due the Van der Waals interactions. For instance, the energy gap difference (Table 2) is very similar to the SWZNT-c(1 1 1) and SWZNT-c (1 1 1)/CO_2 complex, SWZNT-c(1 1 1)/CH_4, indicating that the adsorption of CO_2 and CH_4 does not significantly alter the electronic properties of SWZNT-c(1 1 1). Consequently, this result suggests that SWZNT-c(1 1 1) is not suitable to be used as a gas sensor to detect CO_2 and CH_4 using electrical conductivity, presenting higher selectivity to the $CFCl_3$ molecule, whose energy gap difference was larger. For example, conductivity can be estimated using Eq. (20) [31].

$$\sigma = e^{\frac{-Eg}{2k_bT}} \tag{20}$$

where, σ is the electrical conductivity, E_g is the energy gap, kb is the Boltzmann constant and T is the temperature. Therefore, the lower value of the E_g implies a higher electrical conductivity.

With favorable E_{ad} and increased conductivity in ~16.17%, these results suggest that SWZNT-c(1 1 1) may be a promising sensor for $CFCl_3$, showing selectivity over other greenhouse gases. Although all gases interact favorably with SWZNT-c(1 1 1), their presence does not significantly affect the density of their HOMO and LUMO energies, as shown in Fig. 3. In detail the most significant change was observed for the formation of the SWZNT-c(1 1 1)/$CFCl_3$ complex, in which the nanotube decreased its LUMO energy density by fixing it on the $CFCl_3$ molecule.

A good chemical sensor should be recovered after work. Thereby, $CFCl_3$ desorption from the surface of nanotubes can be obtained using physical (for example, temperature) and/or chemical processes, because the HOMO and LUMO energies are located only in the $CFCl_3$ molecule in SWZNT-c(1 1 1). MEP analysis shows that $CFCl_3$, CO_2, CH_4 adsorbed on the nanotube does not significantly change their electrostatic surfaces (see Fig. 4). The main changes observed are due to the charge transfer of $CFCl_3$ and CO_2 to the −0.12 and −0.03e- nanotubes, respectively.

5. Conclusions

At this work, the DFT method was used to study the adsorption of polluting gases ($CFCl_3$, CO_2 and CH_4) in SWZNT-c(1 1 1), with the intention of obtaining a new gas sensor for polluting agents. The SWZNT-c(1 1 1) structure is preserved throughout the adsorption process. The adsorption energy indicates that the interaction between the gases and the nanotube is a favorable process, whose SWZNT-c(1 1 1) interacting with $CFCl_3$ has the lowest E_{ad} with a value of −3.08 kcal / mol. The Eg analysis showed that SWZNT-c(1 1 1) cannot be used as a gas sensor (CO_2 and CH_4) based on conductivity, showing selectivity for the $CFCl_3$ molecule, observing a ~ 16.17% variation in conductivity throughout the adsorption process. Therefore, the SWZNT-c(1 1 1) is more suited to be a new gas sensor for the $CFCl_3$ molecule. Overall, our theoretical results obtained here can be used to support future theoretical and experimental studies on the use of SWZNT-c(1 1 1) as a green house gas detector.

Declaration of Competing Interest

The authors declare that they have no known competing financial interests or personal relationships that could have appeared to influence the work reported in this paper.

Acknowledgements

This research was conducted with the support of the High Performance Computing Center of the State University of Goiás. José Antônio Pinheiro Lobo also recognizes the Coordination of Higher Education Personnel Improvement (CAPES) for the granting of a scholarship.

References

[1] Y.Q. Hongtao Gao, Jing Zhou1 Dongmei Dai, Photocatalytic Activity and Electronic Structure Analysis of N-doped Anatase TiO2: A Combined Experimental and Theoretical Study, Chem. Eng. Technol. (2009) 867–872, https://doi.org/10.1002/ceat.200800624.
[2] A.A.G. Santiago, N.F. Andrade Neto, E. Longo, et al., Fast and continuous obtaining of Eu3 + doped CeO2 microspheres by ultrasonic spray pyrolysis : characterization and photocatalytic activity, J. Mater. Sci. Mater. Electron. 30 (2019) 11508–11519, https://doi.org/10.1007/s10854-019-01506-7.
[3] W. An, Y. Pei, X.C. Zeng, CO Oxidation Catalyzed by Single-Walled Helical Gold Nanotube, NANO Lett. 9 (2008) 195–202.
[4] W. Qin, X. Li, A theoretical study on the catalytic effect of nanoparticle confined in carbon nanotube, Chem. Phys. Lett. 502 (2011) 96–100, https://doi.org/10.1016/j.cplett.2010.12.030.
[5] M. De Jesus, S. Chaves, D. Oliveira, M. De Assis, T. Cristina, S. Franco, Journal of Solid State Chemistry Environmental remediation properties of Bi2 WO6 hierarchical nanostructure : a joint experimental and theoretical investigation, J. Solid State Chem. 274 (2019) 270–279, https://doi.org/10.1016/j.jssc.2019.03.031.
[6] M. Assis, E. Cordoncillo, R. Torres-mendieta, H. Beltrán-mir, G. Mínguez-vega, R. Oliveira, E.R. Leite, C.C. Foggi, C.E. Vergani, E. Longo, J. Andrés, Towards the scale-up of the formation of nanoparticles on α -Ag2WO4 with bactericidal properties by femtosecond laser irradiation, Sci. Rep. (2018) 1–11, https://doi.org/10.1038/s41598-018-19270-9.
[7] J. Rodrigues, E. Longo, O. Vital, D. Oliveira, Theoretical study of sarin adsorption on (12,0) boron nitride nanotube doped with silicon atoms, Chem. Phys. Lett. 738 (2020) 136816, , https://doi.org/10.1016/j.cplett.2019.136816.
[8] D.C. Sorescu, K.D. Jordan, P. Avouris, Theoretical Study of Oxygen Adsorption on Graphite and the (8,0) Single-walled Carbon Nanotube, J. Phys. Chem. 11227–11232 (2001).
[9] A. Salomonsson, R.M.P. Jr, K. Uvdal, C. Aulin, P. Ka, M. Strand, M. Sanati, A.L. Spetz, Nanocrystalline ruthenium oxide and ruthenium in sensing applications – an experimental and theoretical study, J. Nanoparticle Res. 1 (2006) 899–910, https://doi.org/10.1007/s11051-005-9058-1.
[10] N.L. Hadipour, A.A. Peyghan, H. Soleymanabadi, Theoretical Study on the Al-Doped ZnO Nanoclusters for CO Chemical Sensors, J. Phys. Chem. 1–32 (2015).
[11] D. Gu, H. Baumgart, G. Namkoong, Atomic Layer Deposition of ZrO2 and HfO2 Nanotubes, Electrochem. Solid-State Lett. 12 (2009) 25–28, https://doi.org/10.1149/1.3070617.
[12] J. Cerd, S. Gallego, J.I. Beltr, Adhesion at metal – ZrO2 interfaces, Surf. Sci. Rep. 61 (2006) 303–344, https://doi.org/10.1016/j.surfrep.2006.03.002.
[13] A. Meldrum, L.A. Boatner, R.C. Ewing, Nanocrystalline Zirconia Can Be Amorphized by Ion Irradiation, Phys. Rev. Lett. 88 (2002) 1–4, https://doi.org/10.1103/PhysRevLett. 88.025503.
[14] S. Iijima, Helical microtubules of graphitic carbon, Lett. to Nat. 354 (1991) 56–58.
[15] E. Artacho, D. Sa, A. Rubio, P. Ordejo, Ab initio structural, elastic, and vibrational properties of carbon nanotubes, Phys. Rev. B 59 678–688 (1999) /Users/erik/Dropbox/scientific_literature/Sa?nchez-Portal_Phys._Rev._B_1999.pdf.
[16] L. Guo, J. Zhao, X. Wang, X. Xu, H. Liu, Y. Li, Structure and Bioactivity of Zirconia Nanotube Arrays Fabricated by Anodization, Appl. Ceram. Technol. 641 (2009) 636–641, https://doi.org/10.1111/j.1744-7402.2008.02305.x.
[17] C. Bae, H. Yoo, S. Kim, K. Lee, J. Kim, M.M. Sung, H. Shin, Template-Directed Synthesis of Oxide Nanotubes : Fabrication, Characterization, and Applications, Chem. Mater. 20 (2008) 756–767.

[18] A.V. Bandura, R.A. Evarestov, Ab initio structure modeling of ZrO2 nanosheets and single-wall nanotubes, Comput. Mater. Sci. 65 (2012) 395–405, https://doi.org/10.1016/j.commatsci.2012.08.001.
[19] I.D. Muhammad, M. Awang, O. Mamat, K. Zilati, K. Shaari, Estimating Young ' s Modulus of Single-Walled Zirconia Nanotubes Using Nonlinear Finite Element Modeling, J. Nanomater. 2 (2015) 1–8.
[20] Hao Cui, Guozhi Zhang, Xiaoxing Zhang, Ju Tang, Rh-doped $MoSe_2$ as toxic gas scavenger: a first-principles study, Nanoscale Adv. 1 (2019) 772.
[21] Hao Cui, Xiaoxing Zhang, Yi Li, Dachang Chen, Ying Zhang First-principles insight into Ni-doped InN monolayer as a noxious gasesscavenger, Appl. Surf. Sci. 494 (2019) 859–866.
[22] Hao Cui, Xiaoxing Zhang, Jun Zhag, Ying Zhang, Nanomaterials-based gas sensors of SF6 decomposed species for evaluating the operation status of high-voltage insulation devices, High Volt. 4 (4) (2019) 242–258.
[23] J.J.P. Stewart, Stewart Computational Chemistry (2016).
[24] K.D. Dobbs, W.J. Hehre, Molecular-orbital theory of the properties of inorganic and organometallic compounds. 6. Extended basis-sets for 2nd-row transition-metals, J. Comp. Chem. 8 (1987) 880–893.
[25] S. Grimme, J. Antony, S. Ehrlich, H. Krieg, A consistent and accurate ab initio parameterization of density functional dispersion correction (DFT-D) for the 94 elements H-Pu, J. Chem. Phys. 132 (2010).
[26] J.R. [M. J. Frisch, G. W. Trucks, H. B. Schlegel, G. E. Scuseria, M. A. Robb, X. Cheeseman, G. Scalmani, V. Barone, B. Mennucci, G. A. Petersson, H. Nakatsuji, M. Caricato, K. Li, H. P. Hratchian, A. F. Izmaylov, J. Bloino, G. Zheng, J. L. Sonnenberg, M. Hada, M. Ehara, T.V. Toyota, R. Fukuda, J. Hasegawa, M. Ishida, T. Nakajima, Y. Honda, O. Kitao, H. Nakai, K.N.K. J. A. Montgomery, Jr., J. E. Peralta, F. Ogliaro, M. Bearpark, J. J. Heyd, E. Brothers, S.S. V. N. Staroverov, R. Kobayashi, J. Normand, K. Raghavachari, A. Rendell, J. C. Burant, V.B. Iyengar, J. Tomasi, M. Cossi, N. Rega, J. M. Millam, M. Klene, J. E. Knox, J. B. Cross, C. C. Adamo, J. Jaramillo, R. Gomperts, R. E. Stratmann, O. Yazyev, A. J. Austin, R. Cammi, J. Pomelli, J. W. Ochterski, R. L. Martin, K. Morokuma, V. G. Zakrzewski, G. A. Voth, P. Salvador, J.C. J. Dannenberg, S. Dapprich, A. D. Daniels, Ö. Farkas, J. B. Foresman, J. V. Ortiz, W.C. 2009.]. and D. J. Fox, gaussian 09, Revision C.01, Gaussian, Inc., gaussian 09, (n.d.).
[27] A.E. Reed, R.B. Weinstock, F. Weinhold, Natural population analysis, J. Chem. Phys. 83 (1985) 735–746, https://doi.org/10.1063/1.449486.
[28] T. Koopmans, UBER DIE ZUORDNUNG VON WELLENFUNKTIONEN UND EIGENWERTEN ZU DEN, EINZELNEN ELEKTRONEN EINES ATOMS, Physic. 1 (1934) 104–113.
[29] M. Sheikhi, S. Shahab, M. Khaleghian, F.H. Hajikolaee, I. Balakhanava, R. Alnajjar, Adsorption Properties of the Molecule Resveratrol on CNT(8,0–10) Nanotube: Geometry Optimization, Molecular Structure, Spectroscopic (NMR, UV/Vis, Excited State), FMO, MEP and HOMO-LUMO Investigations, J. Mol. Struct. (2018), https://doi.org/10.1016/j.molstruc.2018.01.005.
[30] M. Khaleghian, F. Azarakhshi, Theoretical modelling of encapsulation of the Altretamine drug into BN (9, 9–5) and AlN (9, 9–5) nano rings : a DFT study, Mol. Phys. (2019) 1–11, https://doi.org/10.1080/00268976.2019.1574987.
[31] S.S. Li, Semiconductor Physical Eletronics, Springer Science & Business Media, 2012.